

# Elaboration of self-coating alumina-based porous ceramics

Laurent Gremillard · Romaric Casadei ·  
Eduardo Saiz · Antoni P. Tomsia

Received: 5 July 2005 / Accepted: 20 October 2005 / Published online: 3 August 2006  
© Springer Science+Business Media, LLC 2006

**Abstract** Materials used for bone substitution (i.e. hydroxyapatite and calcium phosphate) are highly successful, since when implanted they provide an efficient scaffold that can be colonized by the patient's bone. However, their poor mechanical properties impede their use for load-bearing applications. In contrast, no material with high mechanical properties also presents a high bioactivity. A possible way of finding a material both strong and bioactive is to use a composite. We propose here a composite deriving its strength from its alumina core and its bioactivity from a calcium phosphate surface. Ceramic scaffolds have been produced by infiltration of polymer open-celled foams. Several compositions of the slurries have been tested, leading to the realization of porous pieces with a biocompatibility gradient at a micrometric scale. The mechanical properties of several new materials are presented and correlated to their microstructure.

## Introduction

Bone substitutes are used in every application when natural bone is missing. This includes bone filling

after the removal of a tumor or around orthopedic implants, tibial inserts (in the case of tibial osteotomy), cranio-facial reconstruction, etc. They are made of porous ceramics that mimic as well as possible the bone architecture and chemical composition. Hydroxyapatite,  $\beta$ -tricalcium phosphate and biphasic calcium phosphates are the most frequently used synthetic materials for bone substitution. Their compositions, being very close to the mineral part of bone, present very good osseo-conductivity. However, their mechanical properties are very low, and they cannot be used alone for load-bearing applications such as tibial osteotomy (they are used in combination with metallic plates and screws that ensure the integrity of the tibia until the bone is re-grown in the calcium phosphate insert). Even handling of the bone substitutes by the surgeons is difficult (surgeons often have to cut the substitutes to the right shape, which leads more often than not to a fracture of the substitute). No material with both good mechanical and good biological properties exists. However, keeping in mind that bioactivity is more a surface property and mechanical properties are due to the bulk, it is possible to conceive a functionally graded composite deriving its strength from a strong, bio-inert core (like alumina or zirconia) and its bioactivity from a calcium phosphate coating. This concept is already in use (titanium hip stems coated with hydroxyapatite for example), but is not often applied to porous materials for which the use of classical methods to obtain coating (such as plasma spray deposition) is impossible.

Many techniques exist to produce cellular ceramics. They can be made by gel casting, where ceramic slurries suspended in a monomeric solution are gelled by

---

L. Gremillard (✉)  
Physical Metallurgy and Materials Sciences Group  
(GEMPPM), National Institute for Applied Science  
(INSA), Lyon, France  
e-mail: laurent.gremillard@insa-lyon.fr

R. Casadei · E. Saiz · A. P. Tomsia · L. Gremillard  
Materials Sciences Division, Lawrence Berkeley National  
Laboratory, Berkeley, CA, USA

in-situ polymerization [1, 2], addition of porogenic agents [3], rapid prototyping with indirect fuse deposition [4], foaming of aqueous slurries [5], infiltration of open-celled polymer foams [6, 7], foaming of pre-ceramic polymers followed by ceramisation [8] or other processes [9–12].

In this work, we chose to process cellular alumina whose struts are coated with tri-calcium phosphate. The ceramic scaffolds have been produced by infiltration of polymer open-celled foams. Several compositions of the slurries have been tested, leading to the realization of scaffolds with a biocompatibility gradient. The mechanical properties of several new materials were measured and correlated to their microstructure.

## Experimental procedures

### Slurries

Alumina-based slurries (Ceralox HPA05,  $d_{50}$ : 0.4  $\mu\text{m}$ , specific area 9  $\text{m}^2 \text{g}^{-1}$ ) of different compositions have been prepared. Various amounts (1, 2, 5, 10 and 20 wt%) of sub-stoichiometric tricalcium phosphate ( $\beta$ -TCP—Fluka) have been added to some of the alumina slurries. This calcium-defective TCP presents a eutectic at 1287  $^\circ\text{C}$ , and thus allows liquid phase sintering of the alumina. A dry content up to 75 wt% in water was achieved through the use of a dispersant (Darvan C, 1.7  $\text{mg m}^{-2}$ ) and 24 h ball milling with 5 mm alumina balls. The slurries exhibited a Newtonian behavior between 0 and 1500  $\text{s}^{-1}$ , with a viscosity between 15 and 20 mPa s.

### Infiltration of the polymer foam

Different polymer foams have been tested for infiltration (several types of polyurethane (100 ppi, density ranging from 30 to 100  $\text{kg m}^{-3}$ ) and melamine (250 ppi, density 10  $\text{kg m}^{-3}$ ). Cracking of the cellular ceramics during sintering occurred with most of the foams. The best candidate was a melamine foam (McMaster-Carr, USA), whose high porosity and thin, needle-like struts allowed the avoidance of cracking during the sintering. Pieces were cut out of 2.5 cm-thick sheets of this foam, and a controlled amount of slurry was poured inside them. The amount of slurry was calculated so that the porosity of the cellular ceramic after sintering was  $\sim 70$  vol%. The infiltrated pieces were then compressed repeatedly ( $\sim 5$  times depending on the size of the piece) to 10% of their initial thickness with a wooden roller, so as to achieve better homogeneity [13].

### Sintering

The thermal cycle was chosen to allow good densification of all the samples, even those without calcium phosphate addition. A first, slow heating (50  $^\circ\text{C/h}$ ) was followed by a 5 h plateau at 600  $^\circ\text{C}$  in order to burn the melamine foam. A second plateau led to the final cellular ceramic (2 h 30 min at 1650  $^\circ\text{C}$ , heating and cooling ramps of 300  $^\circ\text{C/h}$ ).

### Characterization

X-ray diffraction (Siemens D5000 diffractometer) allowed identification of the different phases. These chemical analyses were confirmed by scanning electron microscopy observations (ISI DS-130C operating at 15 kV coupled with an EDAX spectrometer for conventional SEM, and Hitachi 4300 FE/N coupled with a Noran EDS analyser for low-vacuum SEM). Due to the difficulty of obtaining a continuous conductive coating on such a highly porous material as our cellular ceramics, low-vacuum SEM appeared to be the ideal tool for the microstructural observations.

The mechanical characterization was made using an Instron testing machine in a compression configuration on  $8 \times 8 \times 8 \text{ mm}^3$  cubes (this geometry was preferred because of the difficulty to obtain nicely shaped cylinders). These dimensions were chosen to avoid any size effect (the biggest microstructural feature, which is the macropores diameter, is  $\sim 200 \mu\text{m}$ ) while allowing easy machining. The porous ceramics were embedded in paraffin prior to machining, in order to strengthen them and to avoid pollution by the cutting fluids. Paraffin was removed prior to mechanical testing by heating the samples in boiling water, followed by a thermal treatment in air (400  $^\circ\text{C}$ , 2 h). Approximately 20 samples of each composition were tested.

## Results

### Microstructure

Pure alumina foams were elaborated first. The effect of the dry content of the alumina slurry on the structure of the cellular ceramic was examined (Fig. 1). Too low dry contents lead to highly porous and microcracked material, and the initial structure of the polymer foam is almost lost. The pieces offer no mechanical resistance. At first sight, the alumina content in the slurries should be no smaller than 60 wt% to obtain good samples. The thermal treatment described above produced almost fully dense walls between the cells

**Fig. 1** Cellular alumina from (a) 75 wt% and (b) ~45 wt%  $\text{Al}_2\text{O}_3$  slurries

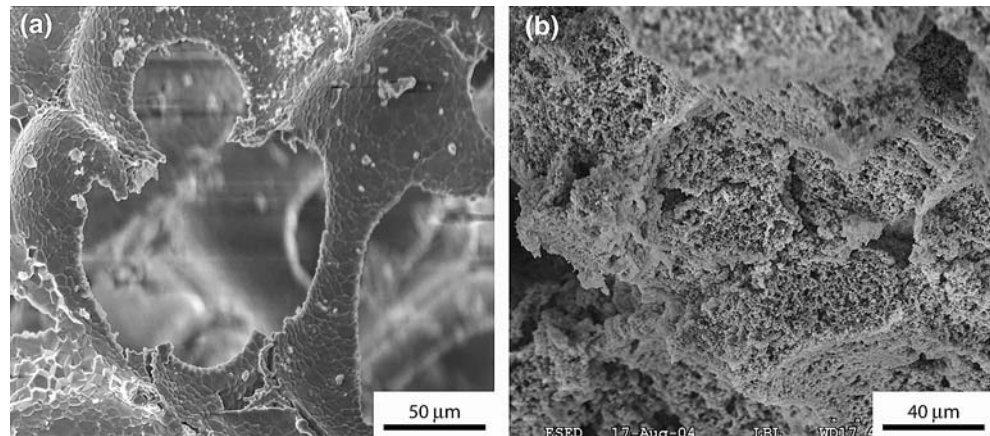


(Fig. 1(a)). However large defects remain, which are due to the elimination of the polymer: when burning, the polymer foam leaves voids that cannot be filled by the ceramic during sintering (Fig. 2).

The major interest of the melamine foam is that it is composed of small-diameter polymer struts (around 5  $\mu\text{m}$ ) as compared to the polyurethane foams (diameter above 50  $\mu\text{m}$ , Fig. 3). Thus the voids formed in the ceramic walls are much smaller, and then susceptible to be filled during liquid phase sintering. Such a sintering can be achieved by adding a sintering aid, namely sub-stoichiometric  $\beta$ -tricalcium phosphate.

Thus  $\beta$ -TCP/alumina bulk samples have been elaborated by slip casting in plaster molds, and subjected to the same thermal treatment as the pure alumina. They were then polished with a 1  $\mu\text{m}$  diamond paste, and thermally treated for 30 min at 1550  $^\circ\text{C}$ . Patches of TCP a few micrometers thick can be seen on the surface of all the samples (Fig. 4). The calcium phosphate surface coverage was determined by image analyses on 10 images per composition, with the software *Image-Tool* from the *University of Texas San Antonio* [14]. It increases with the  $\beta$ -TCP content up to 5 wt%, and

then seems to decrease slightly (Fig. 5). The microstructure is highly porous for high TCP contents. The presence of  $\alpha$ -TCP in some of the composites is noticeable (Fig. 6).

The same coating can be observed on the cellular ceramics (Fig. 7). Only the coating is much thinner (less than 1  $\mu\text{m}$ ), and more TCP is needed to achieve the same coverage. Indeed, no TCP coating could be observed for TCP contents smaller than 20 wt%. As in the case of the bulk samples, the densification of the TCP-doped ceramics is not complete, in spite of the high sintering temperature.

#### Mechanical properties

The strengths of the different materials were evaluated in compression. The evolution of  $\sigma_f$  with the TCP content shows two parts (Fig. 8(a)): first a decrease of the strength with increasing TCP content until 10 wt%, where the strength is very low (average around 4 MPa). This is followed by an increase of the fracture stress, which reaches an average of 12 MPa for 20% TCP. However these values should be considered very

**Fig. 2** “Memory” of the polymer, resulting (a) in ~2  $\mu\text{m}$  wide defects in the cellular ceramic obtained from the melamine foam, or (b) in ~20  $\mu\text{m}$  wide defects in the ceramic obtained from polyurethane foam

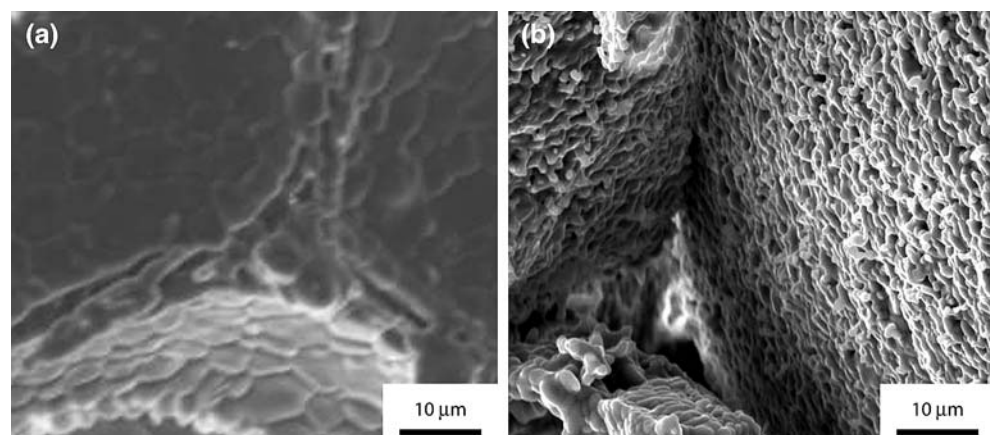
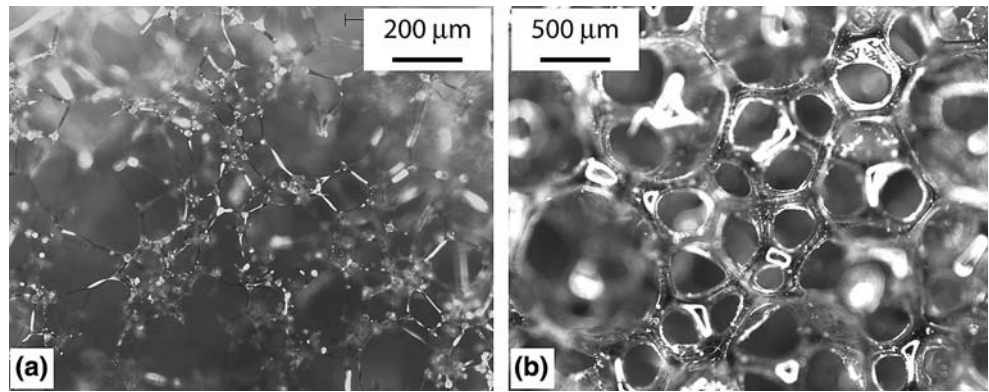


**Fig. 3** (a) Melamine foam, with very thin struts ( $\sim 5 \mu\text{m}$  diameter); (b), multiuse polyurethane foam, with struts diameter greater than  $50 \mu\text{m}$



carefully, since the variability is very high (the best samples have strength greater than 30 MPa). The strengths measured on our materials are in good agreement with the literature for cellular alumina with comparable porosities (higher than 70%), especially the samples with the lowest TCP content (0 and 5%).

## Discussion

### Microstructure

The influence of the amount of powder in the slurry is tremendous. A low solid content is very detrimental for the formation of the cellular ceramic. The problems arise during the first stages of the preparation of the foams, i.e. during the infiltration of the polymer foam. To explain what happens, one can calculate the volume occupied by the slurry inside the melamine foam versus the solid loading of the slurry. Considering 20% linear shrinkage during sintering (measured by comparing the dimensions before and after sintering) and neglecting the volume occupied by the melamine struts, it is given by this expression (1):

$$\frac{V_S}{V_f} = d_{\text{ap}}(1-s)^3 \left( 1 + \frac{1-w}{w} \frac{\rho_{\text{Al}_2\text{O}_3}}{\rho_{\text{H}_2\text{O}}} \right) \quad (1)$$

Where  $V_s$  is the volume of slurry necessary to obtain the desired density after sintering,  $V_f$  the volume of polymer foam to infiltrate,  $s$  is the linear shrinkage during sintering (thus  $V_f \times (1-s)^3$  is the volume of cellular ceramic after sintering),  $d_{\text{ap}}$  the apparent density of the cellular ceramic after sintering,  $\rho_{\text{Al}_2\text{O}_3}$  the density of alumina, and  $w$  the dry content of the slurry (in weight). The result is plotted with typical values in Fig. 9. This figure shows that a solid loading of the slurry higher than 43 wt% (vertical line) is absolutely necessary (lower solid loadings would lead

to a volume of slurry higher than the volume of polymer foam, which is practically impossible). Close to 43%, all the volume inside the melamine foam is occupied by the slurry ( $V_s/V_f \sim 1$ ). During drying, many ceramic particles are too far from the polymer struts to reach it and coat it. Thus clusters of ceramic particles form inside the pores of the polymer foam, and the structure of the polymer sponge is lost. If the solid loading is higher than  $\sim 65\%$ , the slurry occupies less than 50% of the volume of the melamine foam ( $V_s/V_f < 0.5$ ). Then, the slurry is mainly supported by the polymer struts or forms bi-dimensional films between the struts, and the center of the porosities is free of slurry. Thus, during drying, a coating of the struts by green ceramic and the formation of dry films occur, but no cluster can form inside the pores. This presents several advantages: the structure of the melamine foam is conserved, implying better mechanical properties since a fully percolating scaffold can be achieved, and the green density of the alumina walls is higher, easing the densification during sintering.

Further densification was achieved through the use of a sintering aid. Indeed, when the melamine foam burns during the sintering cycle, it leaves holes inside the ceramic struts. The melamine foam being formed of very narrow struts (around  $5 \mu\text{m}$ ) these holes can be filled by a liquid phase. The sub-stoichiometric  $\beta$ -TCP (calcium deficient) was chosen as a sintering aid because it shows a eutectic at  $1287 \text{ }^\circ\text{C}$ , and because it is biocompatible, and even an osseo-conductor. The filling of the struts was observed. However, severe microcracking occurred in the composites with a high TCP content (from 5 to 10 wt %), due to the difference of thermal expansion coefficients on the one hand ( $\sim 9 \cdot 10^{-6}$  for alumina,  $\sim 15 \cdot 10^{-6}$  for TCP [15]), and to the extremely low toughness of the  $\beta$ -TCP (less than  $1 \text{ Mpa}\cdot\text{m}^{1/2}$ ) on the other hand. This explains the evolution of the mechanical behavior: there is a competition between the filling of the big pores inside

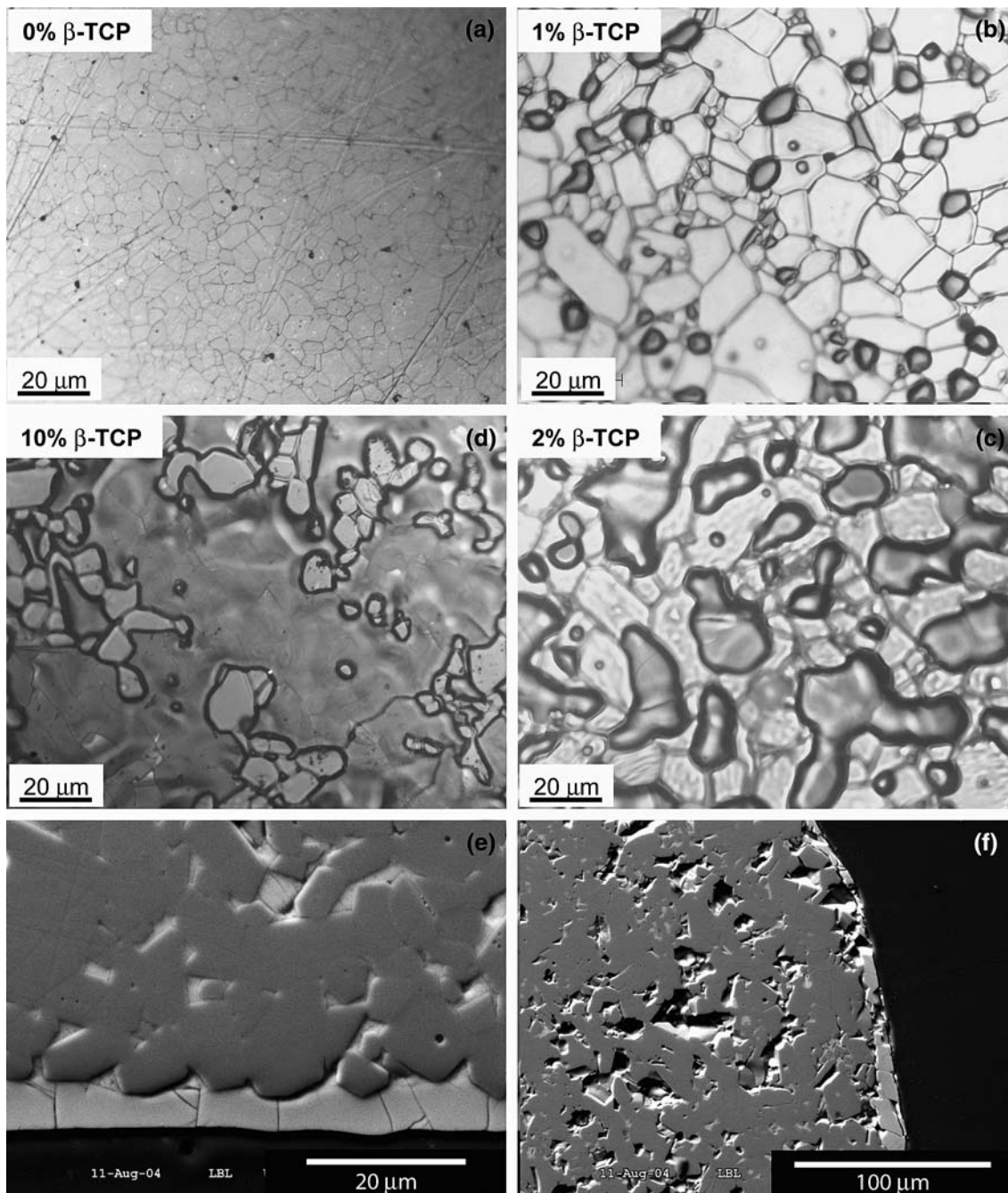


**Fig. 4** Surface of the bulk alumina-TCP samples (0, 1, 2 and 10 wt%  $\beta$ -TCP from (a) to (d)), polished and annealed at 1550 °C for 0.5 h. (e) Cross section of the 10% sample, showing a

~6  $\mu$ m thick TCP layer (bottom). (f) Cross section of the same sample, showing the highly porous microstructure

the struts, and the microcracking. For the lowest TCP contents, the microcracking is predominant, leading to a decrease in strength with increasing TCP content. Above 10 wt%, the filling of the big pores begins to dominate, leading to an increase in strength.

The most interesting feature of these materials is without doubt their ability to cover themselves with a TCP layer. This is very clear on the surfaces of the bulk

materials, where almost continuous TCP coating can be observed. This is less obvious in the cellular materials, where the coating was much more difficult to observe. Nevertheless, on the 20 wt% TCP-alumina, the presence of a non-continuous coating is clear. These different behaviors between the bulk samples and the cellular ceramic may be due to the difference in the specific areas. The bulk samples have a

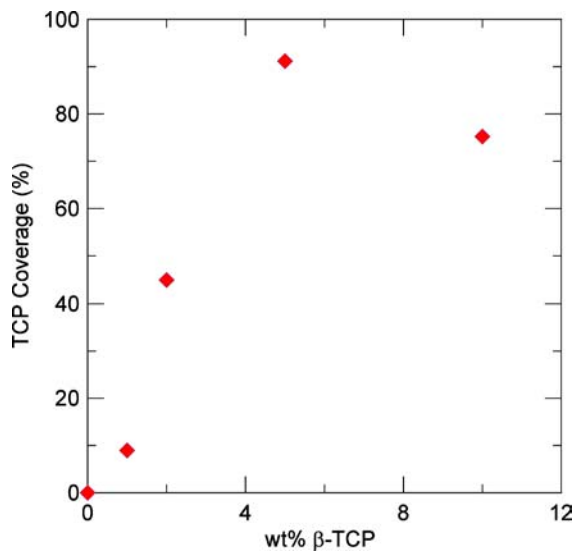


**Fig. 5** Evolution of the TCP coverage on the surface of the bulk samples with the  $\beta$ -TCP content in the slurry

comparatively very small surface, thus all the liquid phase expelled from the alumina core is located on this small surface, leading to thick, almost continuous coatings. For the same volume of material, the surface of the cellular ceramic is several orders of magnitude higher, thus the liquid phase has to spread much more, leading to thin and discontinuous coatings. However, due once more to the difference of the thermal expansion coefficients of the TCP and alumina and to the low toughness of the TCP, cracking of the coating on the bulk samples is obvious. Indeed, considering that the alumina is infinitely rigid compared with the coating (which is most probable, since the alumina piece is several millimeters thick, versus a few micrometers for the coating, and since the Young modulus of alumina is much higher than the modulus

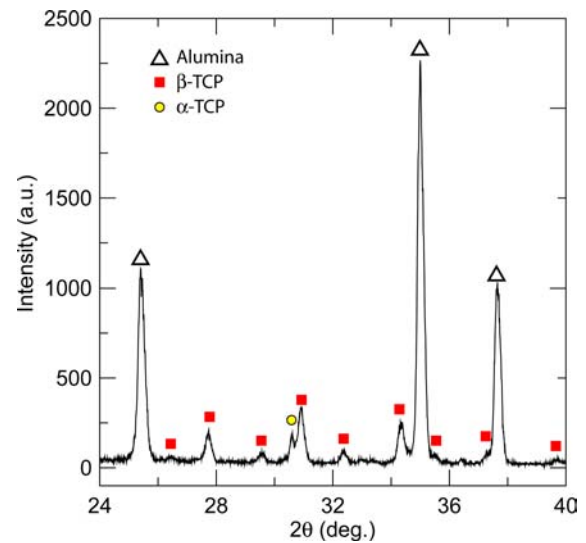


**Fig. 6** XRD analysis of the polished surface of alumina/10 wt%  $\beta$ -TCP sample, showing the presence of  $\alpha$ -TCP (circle),  $\beta$ -TCP (squares) and alumina (triangles)

of TCP (400 vs.  $\sim$ 100 GPa resp. [16–18])), the coating is submitted to a strain  $\varepsilon = \Delta\alpha\Delta T = 0.76\%$ , if one considers that  $\Delta T$  is the difference in temperature between the eutectic temperature of the TCP and room temperature. This corresponds to a stress around 700 MPa, much higher than any strength measured for TCP, and consequently explains the microcracking of the TCP layer. Even in the cellular materials, where the alumina core cannot be considered as infinitely rigid, a cracking of the coating is detected.

Samples similar to ours have been obtained by Jun [19] using a slightly different technique, developed during the last few years [20–21]. The polymer sponge was first impregnated with alumina slurry, then dried and sintered, and impregnated again several times with alumina slurries to increase the density, each

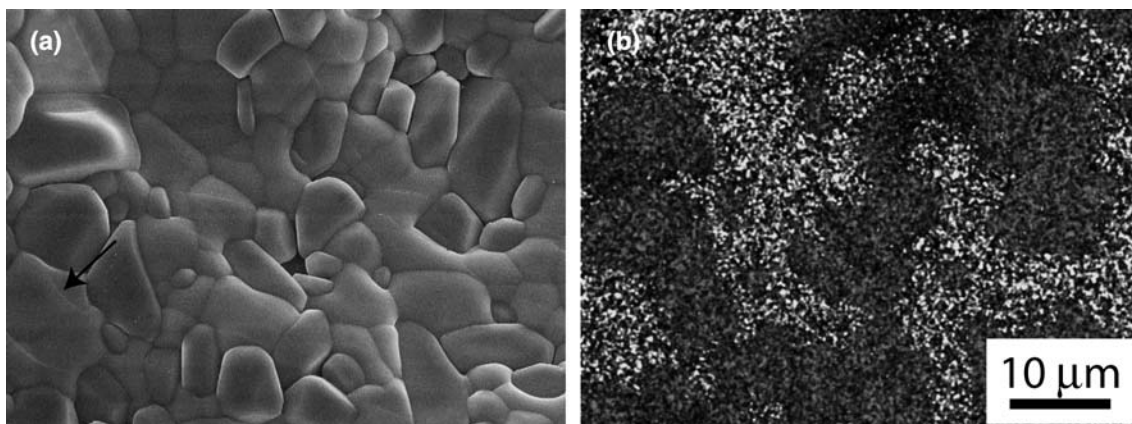


**Fig. 7** Surface of an alveola of alumina-20 wt%  $\beta$ -TCP cellular ceramic; (a) SEM picture, the TCP areas can be recognized because they are slightly cracked (arrows); (b) EDS map of the same area, where the TCP appears in white and the alumina in dark grey

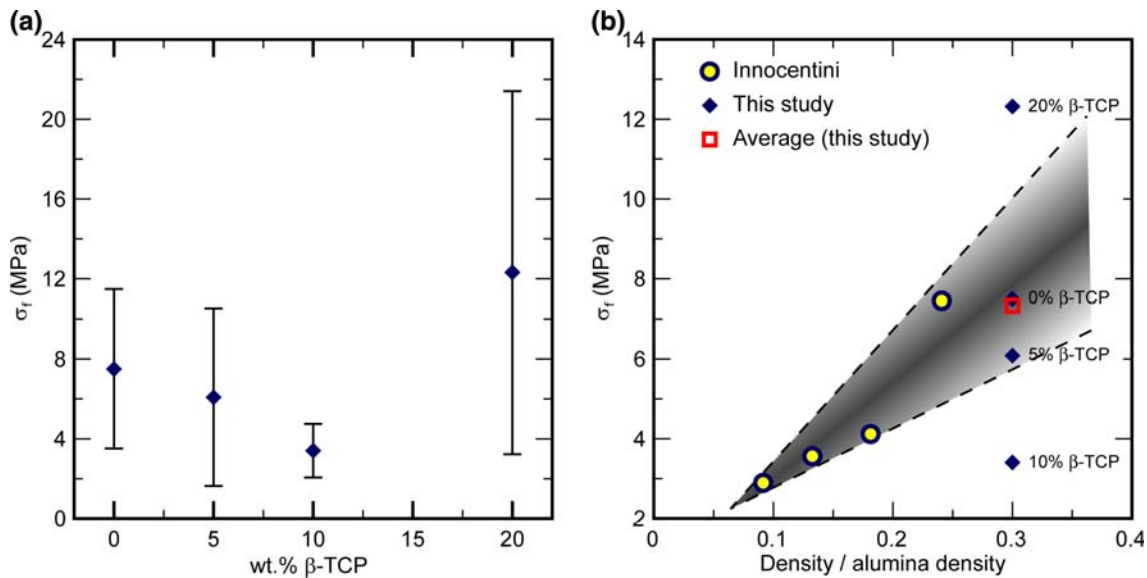


**Fig. 8** (a) Fracture stress vs.  $\beta$ -TCP content in the slurry for the 30% density cellular ceramics; (b) comparison of our materials with values from the literature for various densities

impregnation followed by sintering. Final impregnations were made with TCP or HAP slurries. The advantage is that the coatings are completely continuous and the mechanical properties are a bit higher. On the other hand, the process is much longer and more complicated. Furthermore, the alumina structure in this study is completely continuous, making its resorption in the body impossible. The alumina structure in our materials presents numerous pockets of TCP. These pockets will be slowly dissolved by the body fluids and cells, and thus after a few years the

alumina scaffold is likely to be very progressively eliminated.

## Conclusions

Porous, open-celled, self-coated ceramics with a composition gradient were developed. They derive their strength from an alumina core, and their bioactivity from a calcium phosphate coating. Their mechanical properties were measured and analyzed in view of their microstructure. The evolution of the mechanical properties was explained by a competition between the microcracking of the ceramic struts and the filling of the voids inside the struts. A criterion to obtain a cellular ceramic with dense walls was proposed, taking into account the solid loading of the slurries. More work is needed to optimize these materials, and in particular in-vitro cell culture studies are necessary. We believe that similar processes can be applied to other systems of materials, making possible the fabrication of a range of ceramics with tailored mechanical properties and bioactivity.

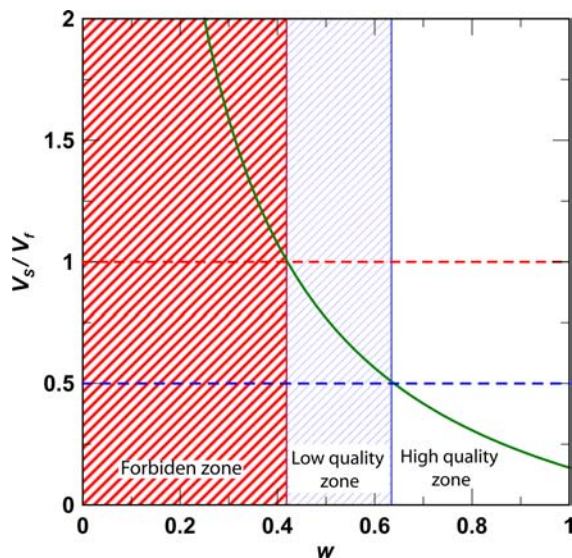


**Fig. 9** Volume of the polymer foam occupied by the slurry against dry content (to obtain a 70% porous cellular alumina (e.g.  $d_{ap} = 1.2 \text{ g cm}^{-3}$ ))

## References

1. Padilla S, Garcia-Carrodeguas R, Vallet-Regi M (2004) J Eur Ceram Soc 24:2223
2. Sepulveda P, Binner JGP, Rogero SO, Higa OZ, Bressiani JC (2000) J Biomed Mater Res 50:27
3. Bignon A, Chouteau J, Chevalier J, Fantozzi G, Carret JP, Chavassieux P, Boivin G, Melin M, Hartmann D (2003) J Mater Sci Materials Medicine 14:89

4. Bose S, Darsell J, Kintner M, Hosick H, Bandyopadhyay A (2003) *Mater Sci Eng C* 23:479
5. Dhara S, Bhargava P (2003) *J Am Ceram Soc* 86:1645
6. Montanaro L, Jorand Y, Fantozzi G, Negro A (1998) *J Eur Ceram Soc* 18:1339
7. Innocentini MDM, Sepulveda P, Salvini VR, Pandolfelli VC (1998) *J Am Ceram Soc* 81:3349
8. Colombo P, Bernardo E (2003) *Compos Sci Technol* 63:2353
9. Thijs I, Luyten J, Mullens J (2004) *J Am Ceram Soc* 87:170
10. Garrn I, Reetza C, Brandesb N, Krohb LW, Schubert H (2004) *J Eur Ceram Soc* 24:579
11. Tang F, Fudouzi H, Sakka Y (2003) *J Am Ceram Soc* 86:2050
12. Lofton CM, Milz CB, Huang H, Sigmund WM (2005) *J Eur Ceram Soc* 25:883
13. Yarwood JC, Dore JE, Kreuss RK, Gray TJ, Pryor MJ (1976) Filtre en mousse céramique, notamment pour la filtration du métal fondu, Brevet français d'invention no. 46 08950
14. Wilcox D, Dove B, McDavid D, Greer D (2004) ImageTool for windows V3.00, <http://ddsdx.uthscsa.edu/dig/itdesc.html>, as on 05 February 2004
15. Nakamura S, Otsuka R (1990) *Termochim Acta* 165:57
16. Gross KA, Bhadang KA (2004) *Biomaterials* 25:1395
17. Rodriguez-Lorenzo LM, Vallet-Regi M, Ferreira JMF, Ginebra MP, Asparicio C, Planell JA (2002) *J Biomed Mater Res* 60:159
18. Roop Kumar R, Wang M (2002) *Mater Sci Eng A* 338:230
19. Jun YK, Kim WH, Kweon OK, Hong SH (2003) *Biomaterials* 24:3731
20. Zhu X, Jiang D, Tan S, Zhang Z (2001) *J Am Ceram Soc* 84:1654
21. Pu X, Liu X, Qiu F, Huang L (2004) *J Am Ceram Soc* 87:1392